THE JOURNAL OF BIOLOGICAL CHEMISTRY VOL. 287, NO. 18, pp. 14606–14614, April 27, 2012

Metabolic and Regulatory Rearrangements Underlying Efficient D-Xylose Utilization in Engineered *Pseudomonas putida* S12*[S]

Received for publication, December 28, 2011, and in revised form, March 6, 2012 Published, JBC Papers in Press, March 13, 2012, DOI 10.1074/jbc.M111.337501

Jean-Paul Meijnen[‡§¶1], **Johannes H. de Winde**[‡§¶2], **and Harald J. Ruijssenaars**[§‖¶]

From the [‡]*Department of Biotechnology, Delft University of Technology, Julianalaan 67, 2628 BC Delft, the* [§]*Bio-Based Sustainable Industrial Chemistry (B-Basic), Julianalaan 67, 2628 BC Delft, the* [¶]*Kluyver Centre for Genomics of Industrial Fermentation, P. O. Box 5057, 2600 GA Delft, The Netherlands, and* [‖]*BIRD Engineering BV, Westfrankelandsedijk 1, 3115 HG Schiedam, The Netherlands*

Background: Metabolic changes associated with an improved D-xylose utilization phenotype were unknown.
Results: Metabolic and regulatory changes of the primary carbon metabolism are responsible for improved D-xylose utilization.
Conclusion: Valuable insight into system-wide rearrangements establishing efficient catabolism of non-natural carbon sources was obtained.
Significance: Multiple targets to rationally engineer and efficiently utilize non-natural carbon sources in industrial microorganisms were identified.

Previously, an efficient D-xylose utilizing *Pseudomonas putida* S12 strain was obtained by introducing the D-xylose isomerase pathway from *Escherichia coli*, followed by evolutionary selection. In the present study, systemic changes associated with the evolved phenotype were identified by transcriptomics, enzyme activity analysis, and inverse engineering. A key element in improving the initially poor D-xylose utilization was the redistribution of 6-phospho-D-gluconate (6-PG) between the Entner-Doudoroff pathway and the oxidative pentose phosphate (PP) pathway. This redistribution increased the availability of 6-PG for oxidative decarboxylation to D-ribose-5-phosphate, which is essential for the utilization of D-xylose via the nonoxidative PP pathway. The metabolic redistribution of 6-PG was procured by modified HexR regulation, which in addition appeared to control periplasmic sugar oxidation. Because the absence of periplasmic D-xylonate formation was previously demonstrated to be essential for achieving a high biomass yield on D-xylose, the aberrant HexR control appeared to underlie both the improved growth rate and biomass yield of the evolved D-xylose utilizing *P. putida* strain. The increased oxidative PP pathway activity furthermore resulted in an elevated NADH/NAD$^+$ ratio that caused the metabolic flux to be redirected from the TCA cycle to the glyoxylate shunt, which was also activated transcriptionally. Clearly, these findings may serve as an important case in point to engineer and improve the utilization of non-natural carbon sources in a wide range of industrial microorganisms.

The utilization of pentose sugars such as D-xylose and L-arabinose by industrial microorganisms is a major issue to be addressed in the quest for efficient bio-based production of fuels and chemicals (1–4). For this reason, much effort has been put into introducing this capacity into industrial production hosts like *Saccharomyces cerevisiae*, *Zymomonas mobilis,* and *Corynebacterium glutamicum* (5–12). In many cases, problems like redox imbalance and partly functional pentose phosphate (PP)[3] pathways are encountered (2, 11–13). These problems illustrate the challenges associated with the pursuit of efficient utilization of non-natural carbon sources, which often requires extensive metabolic and/or regulatory rearrangements. Different approaches may be followed to achieve such systemic adjustments. The "rational approach" involves the introduction of targeted changes based on a design that presupposes detailed knowledge of the microbial system in terms of genetics, physiology, and metabolic networks (14). Alternatively, (parts of) metabolic pathways may be introduced after which the microbial host is subjected to evolutionary selection. This gives the system the opportunity to establish a new stable and optimized state after the perturbation caused by introducing foreign enzyme activities or pathways (10, 15, 16).

Such a semi-targeted approach was employed to obtain an efficient D-xylose utilizing strain of the solvent-tolerant bacterium *Pseudomonas putida* S12. This organism can be employed as a platform host for the production of aromatic compounds from renewable carbon sources like D-glucose and glycerol (17–22). However, since *P. putida* S12 lacks a D-xylose dissimilation

* This work was supported by the Netherlands Ministry of Economic Affairs and the B-Basic partner organizations through B-Basic, a public-private NWO-Advanced Chemical Technologies for Sustainability program.
[S] This article contains supplemental Tables S1 and S2, Data S1, and Fig. S1.
[1] Present address: Laboratory of Molecular Cell Biology, Institute of Botany and Microbiology, KU Leuven, and the Dept. of Molecular Microbiology, Flanders Institute of Biotechnology (VIB), Kasteelpark Arenberg 31, B-3001 Leuven-Heverlee, Flanders, Belgium.
[2] To whom correspondence should be addressed: Dept. of Biotechnology, Delft University of Technology, Julianalaan 67, 2628 BC Delft, the Netherlands. Tel.: 31-15-2786659; Fax: 31-15-2782355; E-mail: J.H.DeWinde@tudelft.nl.

[3] The abbreviations used are: PP, pentose phosphate; D, dilution rate; Xu5P, D-xylulose 5-phosphate; 6-PG, 6-phospho-D-gluconate; ED, Entner-Doudoroff; KDPG, 2-keto-3-deoxy-6-phospho-D-gluconate; Ru5P, D-ribulose 5-phosphate; Ri5P, D-ribose 5-phosphate.

pathway, it is not able to produce these compounds from D-xylose and L-arabinose (23, 24). Because D-xylose is the second most abundant sugar in lignocellulosic materials, we previously introduced the D-xylose isomerase pathway from *Escherichia coli*, which resulted in a strain that metabolized D-xylose via the PP pathway. Subsequent evolutionary selection resulted in substantial improvement of both growth rate and biomass-to-substrate yield (23). It was established that the absence of active D-glucose dehydrogenase accounted for most of the improved biomass yield on D-xylose (23). The molecular basis for the improved growth rate was not clarified, although the strongly improved growth rate on D-xylose indicated that the normally anabolic PP pathway had been transformed into an efficient catabolic route.

Due to the nature of the optimization procedure (by evolutionary selection), the molecular background of the improved phenotype was nonetheless largely obscure. Therefore, the evolved strain *P. putida* S12xylAB2 was analyzed at the transcriptome level to gain more insight into the systemic changes associated with the improved D-xylose utilizing phenotype. Transcriptional changes revealed various important metabolic and regulatory rearrangements associated with the improved D-xylose utilization phenotype, which were verified by an inverse engineering approach. With these results we obtained further understanding of the effects brought about by the evolutionary selection. This may facilitate the design of effective artificial metabolic networks for the utilization of non-natural carbon sources in industrial microorganisms.

EXPERIMENTAL PROCEDURES

Culture Conditions—The strains and plasmids used in this study are shown in supplemental Table S1. *P. putida* S12xylAB2 is an engineered strain expressing the D-xylose isomerase pathway from *E. coli* and was additionally optimized for enhanced D-xylose utilization by evolutionary selection (23). *P. putida* S12xylXAD is a transformant strain that expresses part of the oxidative D-xylose metabolic route from *Caulobacter crescentus* (24). The media used were Luria broth (25) and a phosphate-buffered mineral salts medium, as described previously (26). In the mineral salts medium, 10 mM D-glucose (MMG) or 12 mM D-xylose (MMX) were used as sole carbon sources, unless stated otherwise. Biotin was added to a final concentration of 20 mg/liter for cultivation of S12xylXAD. For expression of genes under control of the *nagAa* promoter (like *gtsA** and *gtsA*BCD*), 0.1 mM sodium salicylate was added as inducer. Antibiotics were added as required, in the following concentrations: gentamicin, 10 μg/ml for mineral salts medium, 30 μg/ml for Luria broth; kanamycin, 50 μg/ml; tetracycline, 30 μg/ml for *P. putida* S12, 10 μg/ml for *E. coli*. Shaker flask experiments were performed in Boston flasks containing 20 ml of mineral salts medium in a horizontally shaking incubator at 30 °C.

For chemostat cultivation, 1-liter fermentors were employed with a BioFlo110 controller (New Brunswick Scientific) containing MMG or MMX. The working volume of the cultures was kept constant at 0.7 liter by continuously removing culture broth. The pH was maintained at 7.0 by automatic addition of 2 M NaOH and the temperature was set at 30 °C. Dissolved oxygen concentrations were kept at 15% air saturation by automatically adjusting the agitation speed. As a inoculum, 35 ml of a late log-phase preculture in MMG or MMX was used. The dilution rate (D) was initially set at 0.05/h until an A_{600} of 1.5 was reached, after which it was gradually increased to a final value of 0.1 or 0.2/h, depending on the strain and medium employed. On MMG, the final D was set at 0.2/h for each tested strain. On MMX, the final D was set at 0.2/h for strain S12xylAB2 and 0.1/h for strain S12xylXAD. The latter strain could not be maintained on MMX at D = 0.2/h, which is in agreement with the low growth rate observed in MMX-grown shaker flask cultures (23, 24). Transcript profiles of *P. putida* S12xylXAD were almost identical in MMG-grown chemostats at D = 0.1/h and 0.2/h and hence, transcriptome profiles at D = 0.1/h and 0.2/h could be safely compared. Cultures were considered to be at steady state when, after at least 5 volume changes, no changes were observed in the carbon source concentration (<50 μM), cell density, and agitation speed.

Microarray Analysis—Transcriptome analyses were performed on steady-state, carbon-limited chemostat cultures (for details, see supplemental Data S1). Sampling from steady-state chemostat cultivations, mRNA isolation, and cDNA preparation for transcriptome analysis were performed as described previously (27). The microarrays used were custom-made high-density microarrays based on the genome sequence of *P. putida* S12.[4] The end-labeled cDNA fragments were hybridized to the microarray according to standard manufacturer's protocols. The hybridized arrays were scanned by ServiceXS (Leiden, The Netherlands) on a high resolution Gene Chip Scanner 3000 7G system with autoloader (Affymetrix) using standard default analysis settings (filter, 570 nm; pixel size, 2.5 μm). The resulting data were imported into Genespring GX software package version 7.3.1 (Agilent Technologies) using the GC RMA algorithm. After normalization of the data, one-way analysis of variance ($p < 0.05$) was used to select genes that changed significantly between the conditions tested.

Construction of Expression Plasmids—Plasmid pBNNmcs(t) (Km) was constructed as follows. The chloramphenicol (Cm) marker from pBBR1mcs was amplified with primers 1 and 2 (supplemental Table S2) as an AvaI/MluI fragment into MluI/Kpn2I (compatible with AvaI) digested pJNNmcs(t) vector (formerly known as pTn-1 (18)). From this plasmid the *nagAa* promotor and Cm marker were amplified using primers 2 and 3 (supplemental Table S2). The resulting PCR fragment was digested using Kpn2I and XmaJI, and ligated in a Kpn2I/XbaI (compatible with XmaJI)-digested pBBR1mcs vector, which resulted in pBNNmcs(t) (Cm). The Cm marker was replaced by a kanamycin (Km) marker obtained by digesting the amplification product of primers 4 and 5 on plasmid pTnMod-KmO with PagI and NcoI and ligation in a PagI- and NcoI-digested pBNNmcs(t)(Cm) vector. This resulted in expression plasmid pBNNmcs(t)(Km).

The gene *gtsA** (the asterisk indicates a mutated copy of *gtsA* from the evolved D-xylose utilizing strain *P. putida* S12xylAB2) and the gene cluster *gtsA*BCD* was amplified by PCR with primers 10–12 (supplemental Table S2) using genomic DNA of

[4] H. J. Ruijssenaars, J. Nijkamp, D. de Ridder, and J. H. de Winde, manuscript in preparation.

strain S12xylAB2. The PCR fragments were subsequently ligated into vector pBNNmcs(t)(Km) using the restriction sites listed in supplemental Table S2. The resulting plasmids were named pBNNgtsA* and pBNNgtsA*BCD.

The *gnd* and *hexR* genes were amplified by PCR using genomic DNA from *P. putida* S12 as the template and oligonucleotide primers 6–9 (supplemental Table S2). The resulting DNA fragments were ligated into vector pBT′mcs (28) using the corresponding restriction sites listed in supplemental Table S2. The resulting plasmids were designated pBT′gnd and pBT′hexR.

Recombinant plasmid pJTxylAB_tkt-tal was constructed by cloning the *tktA-tal* genes from *P. putida* S12 into plasmid pJTxylAB (23). The *tktA* and *tal* genes were amplified by PCR using oligonucleotide primers 13–16 (supplemental Table S2). First, *tktA* was ligated into vector pJTxylAB using restriction sites Bsp120I and NotI. Subsequently, *tal* was ligated into plasmid pJTxylAB_tkt using restriction sites NotI and XmaJI, yielding plasmid pJTxylAB_tkt-tal.

Construction of Knock-out Mutants—*P. putida* S12 knock-out mutants were constructed as described previously (23). Primers used for amplification of the flanking regions of target genes are presented in supplemental Table S2. Gene replacement vectors for *edd* (6-phosphogluconate dehydratase), *eda* (2-keto-3-deoxy-6-phosphogluconate aldolase), *aceA* (isocitrate lyase), *gtsABCD* (D-glucose ABC-transporter), and *hexR* (transcriptional regulator) genes were constructed in pJQ200SK (29). These vectors were used to delete or interrupt selected genes in wild-type *P. putida* S12 and *P. putida* S12xylAB2 by homologous recombination. After confirming deletion of the target gene by PCR and curing the knock-out strain from the antibiotic marker using the cre-loxP system (30, 31), *xylAB* was introduced into the mutant strains to construct the strains listed in supplemental Table S1.

DNA Techniques—Genomic DNA was isolated using the FastDNA kit (Qbiogene). Plasmid DNA was isolated with the QIAprep spin miniprep kit (Qiagen). DNA concentrations were measured with an ND-1000 spectrophotometer (Nanodrop). Agarose-trapped DNA fragments were isolated with the QIAEXII gel extraction kit (Qiagen). PCRs were performed with Accuprime *Pfx* polymerase (Invitrogen) according to the manufacturer's instructions. Plasmid DNA was introduced into electrocompetent cells using a Gene Pulser electroporation device (Bio-Rad). DNA sequencing reactions were performed by Eurofins MWG Operon (Ebersberg, Germany).

Analytical Methods—Optical densities were measured at 600 nm (A_{600}) using an Ultrospec Cell Density Meter (Amersham Biosciences). An optical density of 1.0 corresponds to a cell dry weight of 0.49 g/liter. Sugars and organic acids were analyzed by ion chromatography (Dionex ICS3000 system) as described previously (23).

NAD^+ and NADH concentrations were measured using the EnzyChrom™ NAD^+/NADH Assay Kit (BioAssay Systems) according to the suppliers' instructions. Samples were taken from mid-log phase cultures and prepared following the manufacturer's instructions. The assay is based on an alcohol dehydrogenase cycling reaction, in which the tetrazolium dye 3-(4,5-Dimethylthiazol-2-yl)-2,5-diphenyltetrazolium bromide is reduced by NADH in the presence of phenazine methosulfate. The color intensity of the reduced product, measured at 565 nm, is proportional to the NADH/NAD^+ concentration in the sample. The absorbance was measured in 96-well plates using a TECAN Infinite 200 microplate reader.

Enzyme Assays—Cell extracts for enzyme assays were prepared by sonication of 5 ml of concentrated cell suspensions (0.9 g/liter cell dry weight in 100 mM Tris-HCl buffer, pH 7.5) from overnight cultures. Cell debris was removed by centrifugation and supernatants were desalted using PD-10 desalting columns (GE Healthcare) prior to activity assays.

The activity of 6-phosphogluconate dehydrogenase was determined spectrophotometrically by continuously measuring NADH or NADPH formation at 340 nm, using 6-phosphogluconate as substrate. The assays were performed at 30 °C, in a total volume of 1 ml. The assay mixture contained 100 mM Tris-HCl buffer (pH 7.5), 2.0 mM NAD^+ or $NADP^+$ and cell extract. The reaction was started by adding 6-phosphogluconate to the reaction mixture to a final concentration of 1.0 mM.

RESULTS

Rearrangement of Central Carbon Metabolism Facilitates Efficient D-Xylose Utilization—To identify the metabolic changes associated with the improved D-xylose utilizing phenotype of the evolved strain *P. putida* S12xylAB2, which metabolizes D-xylose via the PP pathway, transcriptomic profiles were determined in steady-state chemostats on D-xylose as the sole carbon source. The nonevolved D-xylose-utilizing strain *P. putida* S12xylXAD, which metabolizes D-xylose oxidatively via the TCA cycle (24), was employed as a control strain. A thorough comparison of these strains was expected to reveal transcriptional effects specifically associated with (optimized). D-xylose utilization via the D-xylose isomerase/PP pathway. In addition, all transcriptomic profiles from D-xylose-grown cultures were compared with profiles of D-glucose-grown cultures, to identify generic effects associated with growth on D-xylose, or with the evolutionary selection procedure. The key findings from the transcriptome comparisons are summarized below; an overview of all differentially expressed genes (fold-change ≥2) is provided in supplemental Data S1. For a schematic representation of the central carbon metabolism of *P. putida* S12, please refer to Fig. 1.

Up-regulation of Pentose Phosphate Pathway—*P. putida* S12xylAB2 converts D-xylose into D-xylulose 5-phosphate (Xu5P) via the introduced D-xylose isomerase pathway. Because Xu5P is further metabolized via the nonoxidative branch of the PP pathway (23), the observed up-regulation of PP pathway genes *tktA* and *tal* was expected (Table 1, Fig. 1). However, the extent of up-regulation was rather modest.

Also the genes of the oxidative branch of the PP pathway (*gnd*, *zwf-2*) were up-regulated. In the oxidative PP pathway, 6-phospho-D-gluconate (6-PG) dehydrogenase (encoded by *gnd*) catalyzes the oxidative decarboxylation of 6-phospho-D-gluconate to D-ribulose 5-phosphate (Ru5P). Ru5P is subsequently isomerized to D-ribose 5-phosphate (Ri5P) by Ru5P isomerase. Thus, the oxidative PP pathway is not directly involved in Xu5P metabolism, but it does provide Ri5P that, in

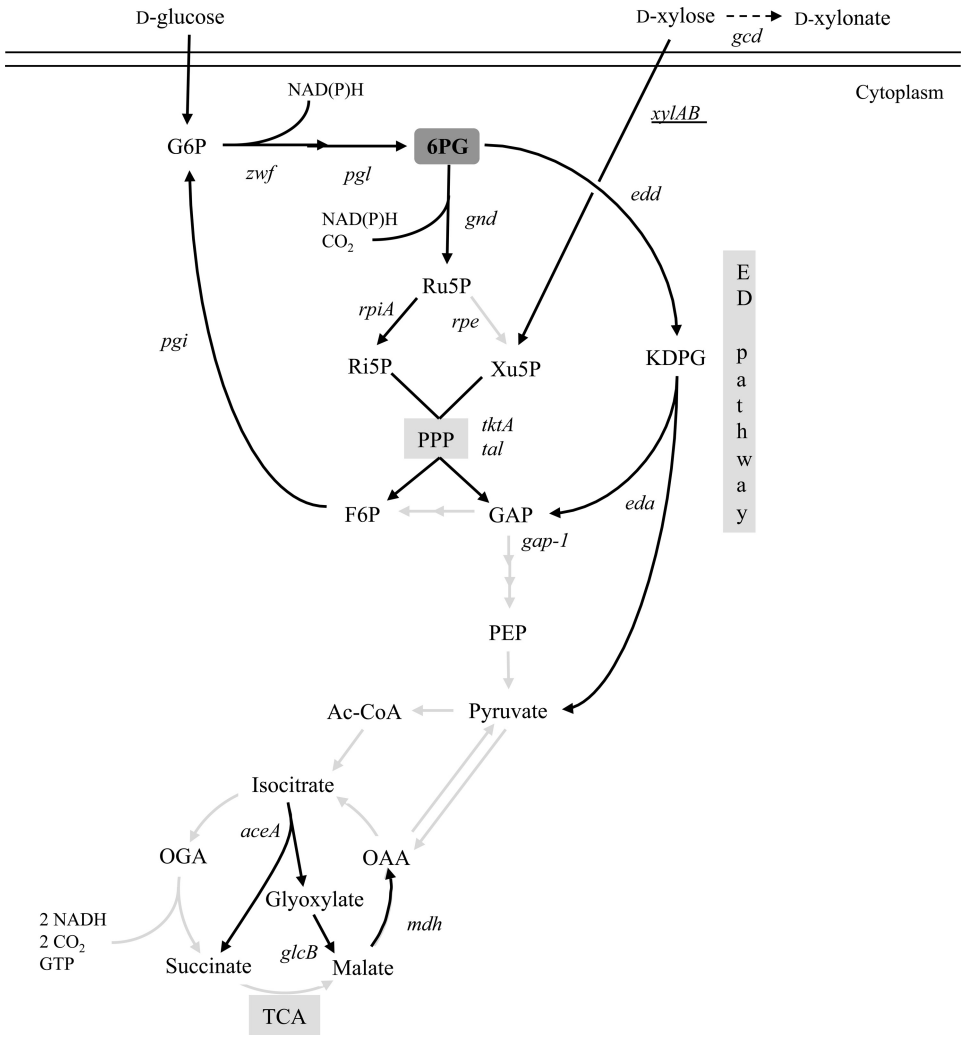

FIGURE 1. **Simplified overview of the central carbon metabolism in *P. putida* S12.** Only metabolic conversions relevant for this study are depicted. *Black arrows* indicate key metabolic conversions involved in the D-xylose metabolism of *P. putida* S12; *gray arrows* indicate conversions that are of minor importance for the D-xylose metabolism. Genes are represented in *italics*. The abbreviations used are: *G6P*, D-glucose 6-P; *F6P*, fructose 6-P; *GAP*, glyceraldehyde 3-P; *PEP*, phosphoenolpyruvate; *Ac-CoA*, acetyl-CoA; *OGA*, 2-ketoglutarate; *OAA*, oxaloacetate; *gcd*, D-glucose dehydrogenase; *zwf*, D-glucose-6-P 1-dehydrogenase; *pgl*, phosphogluconolactonase; *gnd*, 6-phospho-D-gluconate dehydrogenase; *rpiA*, D-ribose-5P isomerase; *rpe*, D-ribulose-5-P epimerase; *tktA*, transketolase; *tal*, transaldolase; *pgi*, phosphoglucoisomerase; *edd*, 6-phosphogluconate dehydratase; *eda*, 2-keto-3-deoxy-6-phospho-D-gluconate aldolase; *gap-1*, glyceraldehyde 3-P dehydrogenase; *aceA*, isocitrate lyase; *glcB*, malate synthase; *mdh*, malate dehydrogenase.

addition to Xu5P, is required to maintain nonoxidative PP pathway fluxes (Fig. 1). Although the *gnd* gene was up-regulated to a relatively limited extent (Table 1), the 6-PG dehydrogenase activity increased from 40 units/g in nonevolved *P. putida* S12xylAB, to 83 units/g in strain S12xylAB2 (Table 2). Also the gene encoding Ru5P isomerase (*rpiA*) was up-regulated. It may be noted that Ru5P can also be produced by direct epimerization of Xu5P. However, the associated *rpe* gene was slightly down-regulated in strain S12xylAB2 (Table 1), which suggested a minor role for this conversion.

Redistribution of 6-PG between PP and ED Pathways—6-Phospho-D-gluconate is the central metabolite of hexose metabolism in Pseudomonads, which is metabolized almost exclusively via the Entner-Doudoroff (ED) pathway (32–33). During growth on D-xylose, however, 6-PG appeared to be the major source of Ri5P in *P. putida* S12xylAB2 as argued above. This implies that part of the 6-PG pool must be redirected from the ED pathway to the oxidative branch of the PP pathway (see also Fig. 1).

The supply of 6-PG is controlled genetically by *zwf-1* and *pgl* genes, which are part of the *eda* operon. The demand for 6-PG in the ED pathway, on the other hand, is controlled by *edd*. A redistribution of the 6-PG pool between the PP and ED pathways may therefore be achieved by tight control of *edd* expression, whereas maintaining or increasing the *zwf-1* and *pgl* expression levels.

Both *eda* operon genes and *edd* were down-regulated during growth on D-xylose (compared with D-glucose), in *P. putida* S12xylAB2 as well as *P. putida* S12xylXAD (Table 1). However, the extent to which these genes were down-regulated and, moreover, their relative expression levels, differed considerably between these two D-xylose utilizing strains. The results clearly show that the *eda* operon genes were up-regulated relative to the *edd* gene in the evolved strain. Moreover, when transcript levels were compared between D-glucose grown *P. putida* S12xylAB2 and D-glucose grown *P. putida* S12pJTmcs (non-D-xylose-utilizing empty vector control), up-regulation of the *eda* operon genes was observed (Table 1). Thus, the evolutionary

TABLE 1
Differentially expressed genes in D-xylose-utilizing strains of *P. putida* S12

	Gene name	Function	Fold-change			
			S12xylAB2 D-xylose *vs.* D-glucose[a]	S12xylXAD D-xylose *vs.* D-glucose[b]	S12xylAB2 *vs.* S12xylXAD D-xylose[c]	S12xylAB2 *vs.* S12pJTmcs D-glucose[d]
edd operon	*gap*	Glyceraldehyde-3P dehydrogenase	0.08	0.09	0.90	-[e]
	edd	6-Phospho-D-gluconate dehydratase	0.20	0.12	1.44	-
	glk	Glucokinase	0.33	0.14	2.03	-
	gltR-2	D-Glucose transporter activator	0.28	0.14	1.84	-
	gtsABCD	D-Glucose ABC-transporter	1.82	0.22	6.34	-
	oprB	Outer membrane porin	1.49	0.34	3.38	-
	hexR	Transcriptional regulator D-glucose metabolism	0.33	0.18	1.68	-
eda operon	*zwf-1*	D-Glucose-6P 1-dehydrogenase	0.33	0.07	4.15	1.63
	pgl	6-Phospho-D-gluconolactonase	0.36	0.06	5.42	1.73
	eda	2-Keto-3-deoxy-6-phospho-D-gluconate aldolase	0.36	0.02	12.2	1.68
PP pathway	*gnd*	6-Phospho-D-gluconate dehydrogenase	1.07	-	1.60	-
	zwf-2	D-Glucose-6P 1-dehydrogenase	1.12	0.62	1.80	-
	tktA	Transketolase	-	-	1.24	-
	tal	Transaldolase	-	-	1.97	-
	rpe	D-Ribulose-5P 3-epimerase	0.89	-	0.94	-
	rpiA	D-Ribose-5P isomerase	1.16	-	1.20	-
Glyoxylate shunt	*aceA*	Isocitrate lyase	5.62	4.80	1.10	-
	glcB	Malate synthase	2.11	1.17	1.58	-
	mdh	Malate dehydrogenase	32.41	125.50	0.12	-
Other	*crp*	Catabolite repressor protein	4.08	4.21	0.95	-
	pqqA	Coenzyme PQQ synthesis protein A	0.50	1.15	0.65	-
	pqqB	Coenzyme PQQ synthesis protein B	0.57	1.43	0.83	-
	pqqC	Coenzyme PQQ synthesis protein C	0.69	1.74	0.39	-
	pqqD	Coenzyme PQQ synthesis protein D	0.77	1.30	0.69	-
	pqqE	Coenzyme PQQ synthesis protein E	0.73	1.37	0.55	-
	pqqF	Coenzyme PQQ synthesis protein F	0.89	1.12	0.92	-

[a] Fold-change in expression level of *P. putida* S12xylAB2 grown on D-xylose compared with D-glucose. Values below 1 represent down-regulation on D-xylose compared with D-glucose; values above 1 represent up-regulation on D-xylose compared with D-glucose.
[b] Fold-change in expression level of *P. putida* S12xylXAD grown on D-xylose compared with D-glucose. Values below 1 represent down-regulation on D-xylose compared with D-glucose; values above 1 represent up-regulation on D-xylose compared with D-glucose.
[c] Fold-change in expression level of D-xylose-grown *P. putida* S12xylAB2 compared with D-xylose-grown *P. putida* S12xylXAD. Values below 1 represent down-regulation in strain S12xylAB2 compared with strain S12xylXAD; values above 1 represent up-regulation in strain S12xylAB2 compared with strain S12xylXAD.
[d] Fold-change in expression level of D-glucose-grown *P. putida* S12xylAB2 compared with D-glucose-grown *P. putida* S12pJTmcs. Values below 1 represent down-regulation in strain S12xylAB2 compared with strain S12pJTmcs; values above 1 represent up-regulation in strain S12xylAB2 compared with strain S12pJTmcs.
[e] Hyphens indicate no differential expression between the tested conditions.

TABLE 2
6-Phospho-D-gluconate dehydrogenase activities of wild-type *P. putida* S12 and evolved D-xylose utilizing *P. putida* S12xylAB2

Activities were measured in cell extracts of D-glucose, respectively, D-xylose-grown cultures of *P. putida* S12 and *P. putida* S12xylAB2, in units/g of protein. 1 unit represents the amount of enzyme that oxidizes 1 μmol of substrate per min. Values are the average of triplicate measurements ± S.D.

Strain and C-source	D-Glucose		D-Xylose	
	NAD^+	$NADP^+$	NAD^+	$NADP^+$
P. putida, S12xylAB	43.1 ± 1.8	6.3 ± 0.9	39.6 ± 1.5	5.8 ± 1.1
P. putida, S12xylAB2	87 ± 6.6	12.4 ± 2.2	83.4 ± 5.4	13.7 ± 2.9

selection strategy apparently brought about an intrinsically altered *eda* operon expression level. Furthermore, the transcript levels of the *edd* operon genes showed a remarkable divergence in D-xylose-grown *P. putida* S12xylAB2: *glk*, *gltR-2*, and *edd* were down-regulated, whereas *gtsABCD* and *oprB* were (mildly) up-regulated.

The differences in transcript levels described above clearly hinted at *edd*- and *eda*-related causes for the discrepancies between the evolved and nonevolved phenotypes of D-xylose utilizing *P. putida* S12. This was confirmed by the growth behavior of *edd* and *eda* deletion mutants (Table 3). In the nonevolved strain, deletion of *edd* resulted in the inability to utilize D-glucose, D-gluconate, or 2-keto-D-gluconate. This defect could not be attributed to the associated interruption of the ED pathway, as deletion of *eda* did not show a similar effect. In the absence of a functional ED pathway, 6-PG should be metabolized via oxidative decarboxylation in the PP pathway (Fig. 1). Thus, the effect of the *edd* deletion may be attributed to the inability to produce 2-keto-3-deoxy-6-phospho-D-gluconate (KDPG; Fig. 1), which is a known inducer of the *edd* and *eda* operons (34, 35). It should be noted that hexose metabolism via the PP pathway requires transcription of additional *edd* and *eda* operon genes, as these encode D-glucose transport (*gtsABCD*, *oprB*), D-glucose phosphorylation (*glk*), and oxidation of Glc-6-P to 6-PG (*zwf-1*, *pgl*). Apparently, KDPG was essential for induction of the *eda* and/or *edd* operons in the nonevolved strain. The evolved strain, however, retained the ability to utilize hexoses upon deletion of *edd*, showing that the "KDPG effect" was lost, or less stringent, in *P. putida* S12xylAB2.

An unexpected observation was the inability of both *edd* and *eda* deletion mutants of *P. putida* S12xylAB2 to utilize D-xylose (Table 3). The deleted genes are clearly not essential for growth on pentoses, as the deletion mutants were able to utilize D-ribose (Table 3). Addition of D-ribose could furthermore relieve the inability to utilize D-xylose for growth.

The up-regulation of the *eda* operon genes relative to *edd*, in addition to the up-regulation of *zwf-2*, suggested that the supply of 6-PG exceeded the demand of the ED pathway in *P. putida* S12xylAB2 during growth on D-xylose. The resulting surplus of 6-PG may then be employed to replenish Ri5P via the oxidative PP pathway branch, establishing the metabolic redistribution of 6-PG as described above. The apparently aberrant role of KDPG in *P. putida* S12xylAB2 indicated that the transcriptional changes of the *edd* and *eda* operons may be the result of a modified transcription control.

TABLE 3

Growth parameters of D-xylose utilizing deletion mutants of evolved and nonevolved *P. putida* S12

Values represent the biomass-to-substrate (Y_{xs}) yield in shake-flask cultures, in cmol % (cmol of CDW/cmol of substrate). The numbers in parentheses indicate the time (h) needed to reach the maximum Y_{xs}. Values are the average of duplicate measurements. The maximum deviation to the average was omitted for clarity, but was always less than 5% of the averaged value.

Strain[a]	Carbon source (60 mmol of C/liter)				
	D-Glucose	D-Xylose	D-Gluconate	2-Keto-D-gluconate	D-Ribose
S12	53 (24)	NG[b]	64 (24)	58 (24)	57 (120)
S12ΔgtsABCD	51 (24)	NG	61 (24)	61 (24)	52 (120)
S12Δedd	NG	NG	NG	NG	32 (216)
S12Δeda	43 (48)	NG	69 (24)	64 (24)	53 (192)
S12ΔaceA	50 (24)	NG	67 (24)	61 (24)	50 (144)
S12xylAB2	44 (24)	67 (24)	61 (24)	43 (24)	60 (120)
S12xylAB2ΔgtsABCD	37 (48)	NG	67 (48)	65 (24)	59 (120)
S12xylAB2Δedd	32 (120)	NG	36 (144)	41 (96)	35 (336)[c]
S12xylAB2Δeda	36 (120)	NG	37 (144)	42 (168)	52 (168)
S12xylAB2ΔaceA	39 (48)	20 (72)	70 (48)	65 (24)	60 (120)

[a] All strains carried the *xylAB* genes from *E. coli* DH5α on plasmid pJT′xylAB.
[b] NG = no growth detected after 240 h. A biomass-to-substrate yield of less than 10 cmol % was regarded as no growth.
[c] Cultivations on D-ribose were prolonged after 240 h because the growth rate on this pentose is intrinsically very low.

D-Xylose Import: Involvement of D-Glucose ABC Transporter—As discussed above, the *gtsABCD* and *oprB-1* genes were up-regulated in *P. putida* S12xylAB2 during growth on D-xylose, in contrast to other genes of the *edd* operon (Table 1). The up-regulated genes encode the D-glucose ABC transporter and the periplasmic porin OprB-1, which is able to transport D-xylose into the periplasm as previously reported for *Pseudomonas aeruginosa* (36). Whereas growth of *P. putida* S12xylAB2 on D-glucose was only marginally affected by deletion of *gtsABCD* (Table 3), growth on D-xylose was completely eliminated, suggesting that D-xylose was imported via the D-glucose ABC transporter. Moreover, sequence analysis of the *gtsABCD* genes in strain S12xylAB2 revealed two mutations in the gene encoding the sugar binding domain (*gtsA*), resulting in amino acid substitutions T74A and P85L (supplemental Fig. S1). These substitutions may result in improved affinity for D-xylose, but this is subject to further investigation. Overexpressing the mutant D-glucose transporter (*gtsA*BCD*) in the nonevolved *P. putida* S12xylAB severely affected growth on both D-xylose and D-glucose, suggesting that overexpression of the transporter compromised the general fitness of the strain.

Up-regulation and Activation of Glyoxylate Shunt—The genes encoding isocitrate lyase (*aceA*), malate synthase (*glcB*), and malate dehydrogenase (*mdh*) were highly up-regulated in D-xylose-grown *P. putida* S12xylAB2 (Table 1), suggesting an active glyoxylate shunt. In addition, an elevated NADH/NAD^+ ratio was observed in D-xylose-grown *P. putida* S12xylAB2 (1.12 *versus* 0.44 in D-glucose grown cells). This condition typically inhibits the activity of isocitrate dehydrogenase, forcing the isocitrate flux toward the glyoxylate bypass (37). The elevated NADH levels likely resulted from the increased oxidative PP pathway activity in *P. putida* S12xylAB2, as the 6-PG dehydrogenase was found to prefer NAD^+ over $NADP^+$ (Table 2). The importance of the glyoxylate shunt for efficient phosphorylative D-xylose metabolism was confirmed by the severely decreased yield and growth rate on D-xylose upon deletion of *aceA* in *P. putida* S12xylAB2 (Table 3).

Down-regulation of PQQ Biosynthesis—A number of genes encoding PQQ biosynthetic enzymes were down-regulated in *P. putida* S12xylAB2 (Table 1). PQQ is the cofactor of D-glucose dehydrogenase, which was found to be inactive during the evolutionary selection of strain S12xylAB2. The inactivity of D-glucose dehydrogenase was found to be the major cause of the improved biomass yield of strain S12xylAB2 on D-xylose (23), and some unclarified post-translational effect was proposed to be involved. This unclarified effect may be associated with the down-regulation of PQQ biosynthesis, because binding of PQQ is essential for constituting an active enzyme (38).

Regulatory Effects Associated with Improved D-Xylose-utilizing Phenotype—The redistribution of the 6-PG pool between the ED and PP pathways appeared to be a key element of the improved D-xylose-utilizing phenotype of *P. putida* S12xylAB2. In addition, the glyoxylate shunt was shown to play an important role, as well as changes relating to D-xylose import and PQQ biosynthesis. These factors appear to characterize most of the improved D-xylose utilization phenotype at the functional level, but do not provide any insight into the regulatory mechanisms behind these changes. Therefore, we specifically mined the transcriptomics dataset for transcriptional changes in, or related to, regulatory genes.

A notable change was observed in the expression of *crp*, encoding the catabolite repression protein Crp (39). The high-level up-regulation of *crp* during growth on D-xylose in *P. putida* S12xylAB2 as well as S12xylXAD (Table 1) clearly illustrated the system-wide derangement provoked by enforcing growth on a non-natural carbon source. In addition, *hexR* was clearly down-regulated in both *P. putida* S12xylAB2 and S12xylXAD during growth on D-xylose, suggesting a generic response associated with growth on D-xylose as observed for *crp*. Down-regulation was less severe, however, in *P. putida* S12xylAB2 (Table 1). The *hexR* gene encodes the key regulator of D-glucose metabolism (34, 35), HexR, through which KDPG exerts its derepressing effect (34, 40). The apparently altered impact of KDPG on transcription of the *eda* and *edd* operons in *P. putida* S12xylAB2 (see above), combined with the relatively mild down-regulation of *hexR* during growth on D-xylose, suggested an important role of HexR (de-)regulation in the improved D-xylose utilizing phenotype.

To obtain more insight into the role of *hexR,* the gene was deleted in the nonevolved D-xylose-utilizing parent of strain S12xylAB2, *P. putida* S12xylAB (23). The growth rate of the resulting strain S12ΔhexR_xylAB was considerably decreased

TABLE 4
Growth parameters of nonevolved, inverse-engineered D-xylose-utilizing *P. putida* S12 strains

Strain	Objective of modification	Yield on D-xylose[a]	Growth rate[b]
		cmol %	*days*
P. putida S12xylAB	Establish growth on D-xylose	14.9 ± 0.5	4[c]
P. putida S12Δgcd_xylAB	Eliminate oxidation of D-xylose	46.5 ± 1.2	7[d]
P. putida S12ΔhexR_xylAB	Derepress D-glucose metabolism	52.9 ± 0.9	13
P. putida S12ΔhexR_xylAB_tkt-tal	Increase capacity of PP pathway	56.0 ± 2.6	3
P. putida S12ΔhexR_xylAB_gnd	Increase supply of D-ribose-5P	19.7 ± 1.0	8
P. putida S12ΔhexR_xylAB_tkt-tal_gnd	Increase supply of D-ribose-5P and increase capacity of PP pathway	25.9 ± 1.3	7
P. putida S12ΔhexR_xylAB_tkt-tal_gtsA*[e]	Increase influx of D-xylose	46.8 ± 1.6	8
P. putida S12ΔhexR_xylAB_tkt-tal_gtsA*BCD	Increase influx of D-xylose	NG[f]	NG

[a] Values are the average of triplicate measurements. Errors represent the S.D.
[b] Number of days required to reach stationary phase when grown on D-xylose.
[c] Because of extensive oxidation of D-xylose, growth stopped after 4 days of incubation.
[d] Results obtained from a previous study (23).
[e] The asterisk indicates a mutated copy of the gene from *P. putida* S12xylAB2 is expressed.
[f] NG, no growth detected.

on D-xylose (Table 4). However, the biomass yield on D-xylose was improved by nearly a factor 4, to 52.9 cmol % (Table 4), which even exceeded the biomass yield achieved by the *gcd* knock-out strain *P. putida* S12Δgcd_xylAB (46.5 cmol %; Table 4). This result strongly suggested that the periplasmic oxidation of D-xylose was affected by deletion of *hexR*. Production of D-xylonate was indeed absent in D-xylose-grown *P. putida* S12ΔhexR_xylAB cultures, whereas the introduction of an episomal copy of *hexR* fully restored D-xylonate formation. It may therefore be concluded that there is a, so far unobserved, connection between HexR and periplasmic sugar oxidation. The nature of this connection appears to be indirect, because an effect of HexR on *gcd* transcription may be excluded based on previous findings in *P. putida* KT2440 (35).

Redistribution of 6-PG Pool by Inverse Engineering—HexR deregulation appeared to be an important feature in establishing efficient D-xylose utilization by *P. putida* S12. However, the dramatically decreased growth rate caused by deleting *hexR* in the nonevolved strain demonstrated that simply eliminating HexR-controlled repression will not establish efficient growth on D-xylose. This observation confirmed our assumption that tight control of *edd* transcription by HexR is essential for proper distribution of 6-PG between the ED and PP pathways.

To establish whether the absence of HexR-control could be counteracted by stimulating the flux of 6-PG to the PP pathway, genes encoding both the oxidative and nonoxidative PP pathway branches were overexpressed in the (nonevolved) *P. putida* S12ΔhexR_xylAB. Overexpression of *gnd* decreased the time required to fully consume 12 mM D-xylose from 13 to 8 days (Table 4). This supported the notion that Ri5P availability limited the growth rate on D-xylose in the *hexR* knock-out strain. The overexpression of *gnd*, however, also resulted in a considerably decreased biomass yield (Table 4). This could likely be attributed to the very high 6-phospho-D-gluconate dehydrogenase activity (3275 ± 291 units/g of protein), which was 37-fold higher than in *P. putida* S12xylAB2 (Table 2). A correspondingly high flux of 6-PG to Ri5P would obviously lead to extensive loss of carbon via CO_2 formation.

Overexpression of *tktA* and *tal* in *P. putida* S12ΔhexR_xylAB was more effective than *gnd* overexpression in improving growth on D-xylose: the time required to consume 12 mM D-xylose was reduced to only 4 days, whereas the biomass yield was unchanged or even slightly improved (Table 4). Apparently, the drain on Ri5P caused by overexpression of the nonoxidative PP pathway stimulated replenishment via the oxidative branch without the negative effect on the biomass yield associated with *gnd* overexpression. When *gnd* was overexpressed in addition to *tktA-tal*, the growth performance was heavily affected: 8 days were required to consume 12 mM D-xylose and the biomass yield dropped to 25.9 cmol %.

DISCUSSION

The molecular background of improved D-xylose utilization by an engineered and evolutionarily selected mutant of *P. putida* S12 was characterized by a combination of system-wide analysis and inverse engineering. Multiple systemic changes were identified that had apparently accumulated under selective pressure for efficient utilization of this unnatural carbon source. Metabolic redistribution of the 6-PG pool appeared to contribute most to the improved growth rate on D-xylose, increasing the availability of 6-PG for the oxidative PP pathway at the expense of the ED pathway. Thus, supply of Ri5P to the nonoxidative PP pathway was ensured, enabling efficient metabolism of D-xylose via Xu5P. Furthermore, we found indications for improved D-xylose import, via the mutated and up-regulated D-glucose ABC-transporter. Expression levels of the nonoxidative PP pathway genes were only slightly elevated. However, as previously reported for *E. coli* (41), small transcriptional changes can significantly alter the PP pathway flux. Such an effect was also observed for *gnd* expression levels and the corresponding 6-PG dehydrogenase activity.

The increased NADH levels, probably resulting from the improved oxidative PP pathway activity, provoked the redirection of the isocitrate flux to the glyoxylate bypass. Historically, the oxidative PP pathway is believed to be associated with NADPH formation. Recent insights, however, show that a preference for NAD^+, as observed for *P. putida* S12, is actually quite common (42). The associated metabolic rearrangement bypasses two CO_2 generating steps of the TCA cycle, adding to the already improved biomass yield caused by the inactive periplasmic sugar oxidation pathway (23). Redistribution of the metabolic flux to the glyoxylate shunt through elevated NADH levels was further sustained by up-regulation of the associated genes in *P. putida* S12xylAB2. In *E. coli*, these genes are con-

trolled by the cAMP-CRP complex (43), suggesting that the observed up-regulation of *crp* accounts for this transcriptional effect.

Modified transcriptional control by HexR, the key regulator of hexose metabolism, appeared to underlie many of the observed changes at the metabolic level. In the evolved strain, the *eda* operon was apparently deregulated, whereas *edd* appeared to be under regular HexR control. This partial deregulation is highly relevant for the engineered *P. putida* S12 that is forced to utilize D-xylose, because it has to cope with the unnatural situation that the PP pathway both demands and supplies 6-PG, via Fru-6-P. A high activity of the ED pathway would considerably reduce 6-PG availability for the PP pathway, leading to further reduction of 6-PG levels because supply is controlled by the PP pathway. This kinetic effect will be exacerbated at the transcriptional level under regular HexR control, as KDPG levels (produced by the ED pathway) will be low when 6-PG is scarce, leading to reduced transcription of the genes encoding the ED pathway as well as the oxidative PP pathway. This vicious cycle can be interrupted by deregulating the *eda* operon while maintaining HexR control on *edd* transcription. Low KDPG levels will only lead to down-regulation of the ED pathway, securing supply of 6-PG via the PP pathway. This appeared to be the case in *P. putida* S12xylAB2, resulting in a stable, self-sustaining redistribution of 6-PG between the ED and PP pathways.

Aberrant HexR control in *P. putida* S12xylAB2 may also be responsible for the divergent regulation of the *edd* operon genes, resulting in the up-regulation of *gtsABCD* and *oprB1* that were shown to be involved in D-xylose import. Moreover, HexR affected the periplasmic sugar oxidation, probably via transcriptional control of PQQ biosynthesis genes. Down-regulation of PQQ biosynthesis would explain inactivation of the periplasmic sugar oxidation pathway in *P. putida* S12xylAB2. The exact mechanism of the altered HexR control remains to be clarified, because no mutations were found in the *hexR* gene itself, or in the promoter regions of the *eda* and *edd* operons.

Efficient D-xylose utilization could not be achieved by simple targeted deletion or overexpression of genes that were found to be differentially expressed in *P. putida* S12xylAB2. Still, these inverse engineering attempts provided valuable insights into the, clearly subtle, metabolic and regulatory changes that were responsible for the optimized D-xylose utilizing phenotype. Although some of the metabolic targets identified in the present study are specific for ED pathway-dependent microorganisms, the generic principles may also be exploited to improve the utilization of non-natural carbon sources by glycolytic microorganisms. Here, the metabolic flux should be controlled at the level of Glc-6-P, rather than 6-PG, as the central node of sugar metabolism. Consequently, phosphoglucose isomerase (Pgi), rather than Edd, may be targeted. Thus, leads for engineering and improving the utilization of non-natural carbon sources were identified that apply to a wide range of industrial microorganisms, and that may contribute to the deployment of renewable, lignocellulosic feed stocks for efficient bioproduction of chemicals and fuels.

Acknowledgments—We thank Hendrik Ballerstedt for performing transcriptomics experiments and Karin Nijkamp for practical assistance. This work was carried out within the research program of the Kluyver Centre for Genomics of Industrial Fermentation, which is part of the Netherlands Genomics Initiative/Netherlands Organization for Scientific Research.

REFERENCES

1. FitzPatrick, M., Champagne, P., Cunningham, M. F., and Whitney, R. A. (2010) A biorefinery processing perspective. Treatment of lignocellulosic materials for the production of value-added products. *Bioresour. Technol.* **101,** 8915–8922
2. Hahn-Hagerdal, B., Karhumaa, K., Fonseca, C., Spencer-Martins, I., and Gorwa-Grauslund, M. F. (2007) Towards industrial pentose-fermenting yeast strains. *Appl. Microbiol. Biotechnol.* **74,** 937–953
3. Lange, J. P. (2007) Lignocellulose conversion; an introduction to chemistry, process and economics. *Biofuels, Bioproducts & Biorefining* **1,** 39–48
4. Octave, S., and Thomas, D. (2009) Biorefinery, toward an industrial metabolism. *Biochimie* **91,** 659–664
5. Deanda, K., Zhang, M., Eddy, C., and Picataggio, S. (1996) Development of an arabinose-fermenting *Zymomonas mobilis* strain by metabolic pathway engineering. *Appl. Environ. Microbiol.* **62,** 4465–4470
6. Kawaguchi, H., Sasaki, M., Vertès, A. A., Inui, M., and Yukawa, H. (2008) Engineering of an L-arabinose metabolic pathway in *Corynebacterium glutamicum*. *Appl. Microbiol. Biotechnol.* **77,** 1053–1062
7. Kawaguchi, H., Vertès, A. A., Okino, S., Inui, M., and Yukawa, H. (2006) Engineering of a xylose metabolic pathway in *Corynebacterium glutamicum*. *Appl. Environ. Microbiol.* **72,** 3418–3428
8. Matsushika, A., Inoue, H., Kodaki, T., and Sawayama, S. (2009) Ethanol production from xylose in engineered *Saccharomyces cerevisiae* strains: current state and perspectives. *Appl. Microbiol. Biotechnol.* **84,** 37–53
9. Van Vleet, J. H., and Jeffries, T. W. (2009) Yeast metabolic engineering for hemicellulosic ethanol production. *Curr. Opin. Biotechnol.* **20,** 300–306
10. Wisselink, H. W., Toirkens, M. J., del Rosario Franco Berriel, M., Winkler, A. A., van Dijken, J. P., Pronk, J. T., and van Maris, A. J. (2007) Engineering of *Saccharomyces cerevisiae* for efficient anaerobic alcoholic fermentation of L-arabinose. *Appl. Environ. Microbiol.* **73,** 4881–4891
11. Yanase, H., Sato, D., Yamamoto, K., Matsuda, S., Yamamoto, S., and Okamoto, K. (2007) Genetic engineering of *Zymobacter palmae* for production of ethanol from xylose. *Appl. Environ. Microbiol.* **73,** 2592–2599
12. Zhang, M., Eddy, C., Deanda, K., Finkelstein, M., and Picataggio, S. (1995) Metabolic engineering of a pentose metabolism pathway in ethanologenic *Zymomonas mobilis*. *Science* **267,** 240–243
13. van Maris, A. J., Winkler, A. A., Kuyper, M., de Laat, W. T., van Dijken, J. P., and Pronk, J. T. (2007) Development of efficient xylose fermentation in *Saccharomyces cerevisiae*. Xylose isomerase as a key component. *Adv. Biochem. Eng. Biotechnol.* **108,** 179–204
14. Lee, J. W., Kim, T. Y., Jang, Y. S., Choi, S., and Lee, S. Y. (2011) Systems metabolic engineering for chemicals and materials. *Trends Biotechnol.* **29,** 370–378
15. Kuyper, M., Toirkens, M. J., Diderich, J. A., Winkler, A. A., van Dijken, J. P., and Pronk, J. T. (2005) Evolutionary engineering of mixed-sugar utilization by a xylose-fermenting *Saccharomyces cerevisiae* strain. *FEMS Yeast Res.* **5,** 925–934
16. Wisselink, H. W., Toirkens, M. J., Wu, Q., Pronk, J. T., and van Maris, A. J. (2009) Novel evolutionary engineering approach for accelerated utilization of glucose, xylose, and arabinose mixtures by engineered *Saccharomyces cerevisiae* strains. *Appl. Environ. Microbiol.* **75,** 907–914
17. Meijnen, J. P., De Winde, J. H., and Ruijssenaars, H. J. (2011) Sustainable production of fine chemicals by the solvent-tolerant *Pseudomonas putida* S12 using lignocellulosic feedstock. *Intl. Sugar J.* **113,** 24–30
18. Nijkamp, K., van Luijk, N., de Bont, J. A., and Wery, J. (2005) The solvent-tolerant *Pseudomonas putida* S12 as host for the production of cinnamic acid from glucose. *Appl. Microbiol. Biotechnol.* **69,** 170–177
19. Nijkamp, K., Westerhof, R. G., Ballerstedt, H., de Bont, J. A., and Wery, J. (2007) Optimization of the solvent-tolerant *Pseudomonas putida* S12 as

host for the production of *p*-coumarate from glucose. *Appl. Microbiol. Biotechnol.* **74,** 617–624
20. Verhoef, S., Ruijssenaars, H. J., de Bont, J. A., and Wery, J. (2007) Bioproduction of *p*-hydroxybenzoate from renewable feedstock by solvent-tolerant *Pseudomonas putida* S12. *J. Biotechnol.* **132,** 49–56
21. Verhoef, S., Wierckx, N., Westerhof, R. G., de Winde, J. H., and Ruijssenaars, H. J. (2009) Bioproduction of *p*-hydroxystyrene from glucose by the solvent-tolerant bacterium *Pseudomonas putida* S12 in a two-phase water-decanol fermentation. *Appl. Environ. Microbiol.* **75,** 931–936
22. Wierckx, N. J., Ballerstedt, H., de Bont, J. A., and Wery, J. (2005) Engineering of solvent-tolerant *Pseudomonas putida* S12 for bioproduction of phenol from glucose. *Appl. Environ. Microbiol.* **71,** 8221–8227
23. Meijnen, J. P., de Winde, J. H., and Ruijssenaars, H. J. (2008) Engineering *Pseudomonas putida* S12 for efficient utilization of D-xylose and L-arabinose. *Appl. Environ. Microbiol.* **74,** 5031–5037
24. Meijnen, J. P., de Winde, J. H., and Ruijssenaars, H. J. (2009) Establishment of oxidative D-xylose metabolism in *Pseudomonas putida* S12. *Appl. Environ. Microbiol.* **75,** 2784–2791
25. Sambrook, J., Maniatis, T., and Fritsch, E. (1982) *Molecular Cloning, A Laboratory Manual*, Cold Spring Harbor Press, Cold Spring Harbor, NY
26. Hartmans, S., Smits, J. P., van der Werf, M. J., Volkering, F., and de Bont, J. A. (1989) Metabolism of styrene oxide and 2-phenylethanol in the styrene-degrading xanthobacter strain 124X. *Appl. Environ. Microbiol.* **55,** 2850–2855
27. Wierckx, N. J., Ballerstedt, H., de Bont, J. A., de Winde, J. H., Ruijssenaars, H. J., and Wery, J. (2008) Transcriptome analysis of a phenol-producing *Pseudomonas putida* S12 construct. Genetic and physiological basis for improved production. *J. Bacteriol.* **190,** 2822–2830
28. Koopman, F., Wierckx, N., de Winde, J. H., and Ruijssenaars, H. J. (2010) Identification and characterization of the furfural and 5-(hydroxymethyl)-furfural degradation pathways of *Cupriavidus basilensis* HMF14. *Proc. Natl. Acad. Sci. U.S.A.* **107,** 4919–4924
29. Quandt, J., and Hynes, M. F. (1993) Versatile suicide vectors which allow direct selection for gene replacement in Gram-negative bacteria. *Gene* **127,** 15–21
30. Sauer, B., and Henderson, N. (1988) Site-specific DNA recombination in mammalian cells by the Cre recombinase of bacteriophage P1. *Proc. Natl. Acad. Sci. U.S.A.* **85,** 5166–5170
31. Sternberg, N., and Hamilton, D. (1981) Bacteriophage P1 site-specific recombination. I. Recombination between loxP sites. *J. Mol. Biol.* **150,** 467–486
32. del Castillo, T., Ramos, J. L., Rodríguez-Herva, J. J., Fuhrer, T., Sauer, U., and Duque, E. (2007) Convergent peripheral pathways catalyze initial glucose catabolism in *Pseudomonas putida*. Genomic and flux analysis. *J. Bacteriol.* **189,** 5142–5152
33. Fuhrer, T., Fischer, E., and Sauer, U. (2005) Experimental identification and quantification of glucose metabolism in seven bacterial species. *J. Bacteriol.* **187,** 1581–1590
34. Daddaoua, A., Krell, T., and Ramos, J. L. (2009) Regulation of glucose metabolism in *Pseudomonas*. The phosphorylative branch and Entner-Doudoroff enzymes are regulated by a repressor containing a sugar isomerase domain. *J. Biol. Chem.* **284,** 21360–21368
35. del Castillo, T., Duque, E., and Ramos, J. L. (2008) A set of activators and repressors control peripheral glucose pathways in *Pseudomonas putida* to yield a common central intermediate. *J. Bacteriol.* **190,** 2331–2339
36. Trias, J., Rosenberg, E. Y., and Nikaido, H. (1988) Specificity of the glucose channel formed by protein D1 of *Pseudomonas aeruginosa*. *Biochim. Biophys. Acta* **938,** 493–496
37. Berg, J. M., Tymoczko, J. L., and Stryer, L. (2002) *Biochemistry*, 5 Ed., W.H. Freeman and Company, New York
38. Matsushita, K., Toyama, H., Ameyama, M., Adachi, O., Dewanti, A., and Duine, J. (1995) Soluble and membrane-bound quinoprotein D-glucose dehydrogenase of the *Acinetobacter calcoaceticus*. The binding process of PQQ to the apoenzymes. *Biosci. Biotech. Biochem.* **59,** 1548–1555
39. Milanesio, P., Arce-Rodríguez, A., Muñoz, A., Calles, B., and de Lorenzo, V. (2011) Regulatory exaptation of the catabolite repression protein (Crp)-cAMP system in *Pseudomonas putida*. *Environ. Microbiol.* **13,** 324–339
40. Kim, J., Jeon, C. O., and Park, W. (2008) Dual regulation of *zwf-1* by both 2-keto-3-deoxy-6-phosphogluconate and oxidative stress in *Pseudomonas putida*. *Microbiology* **154,** 3905–3916
41. Gonzalez, R., Tao, H., Shanmugam, K. T., York, S. W., and Ingram, L. O. (2002) Global gene expression differences associated with changes in glycolytic flux and growth rate in *Escherichia coli* during the fermentation of glucose and xylose. *Biotechnol. Prog.* **18,** 6–20
42. Fuhrer, T., and Sauer, U. (2009) Different biochemical mechanisms ensure network-wide balancing of reducing equivalents in microbial metabolism. *J. Bacteriol.* **191,** 2112–2121
43. Nanchen, A., Schicker, A., Revelles, O., and Sauer, U. (2008) Cyclic AMP-dependent catabolite repression is the dominant control mechanism of metabolic fluxes under glucose limitation in *Escherichia coli*. *J. Bacteriol* **190,** 2323–2330

Metabolic and Regulatory Rearrangements Underlying Efficient d-Xylose Utilization in Engineered *Pseudomonas putida* S12

Jean-Paul Meijnen, Johannes H. de Winde and Harald J. Ruijssenaars

J. Biol. Chem. 2012, 287:14606-14614.
doi: 10.1074/jbc.M111.337501 originally published online March 13, 2012
